

Learning from Pseudo-labeled Segmentation for Multi-Class Object Counting

Jingyi Xu
Stony Brook University
jingyixu@cs.stonybrook.edu

Hieu Le
EPFL
minh.le@epfl.ch

Dimitris Samaras
Stony Brook University
samaras@cs.stonybrook.edu

Abstract

Class-agnostic counting (CAC) has numerous potential applications across various domains. The goal is to count objects of an arbitrary category during testing, based on only a few annotated exemplars. In this paper, we point out that the task of counting objects of interest when there are multiple object classes in the image (namely, multi-class object counting) is particularly challenging for current object counting models. They often greedily count every object regardless of the exemplars. To address this issue, we propose localizing the area containing the objects of interest via an exemplar-based segmentation model before counting them. The key challenge here is the lack of segmentation supervision to train this model. To this end, we propose a method to obtain pseudo segmentation masks using only box exemplars and dot annotations. We show that the segmentation model trained on these pseudo-labeled masks can effectively localize objects of interest for an arbitrary multi-class image based on the exemplars. To evaluate the performance of different methods on multi-class counting, we introduce two new benchmarks, a synthetic multi-class dataset and a new test set of real images in which objects from multiple classes are present. Our proposed method shows a significant advantage over the previous CAC methods on these two benchmarks.

1. Introduction

Class-agnostic counting (CAC) aims to infer the number of objects in an image, given a few object exemplars. Compared to conventional object counters that count objects from a specific category, *e.g.*, human crowds [31], cars [27], animals [3], or cells [38], CAC can count objects of an arbitrary category of interest, which enables numerous applications across various domains.

Most of the current CAC methods focus on capturing the intra-class similarity between image features [23, 32, 30, 14]. For example, BMNet [32] adopts a self-similarity module to enhance the feature’s robustness against intra-class variations. Another recent approach, SAFECOUNT [41], uses

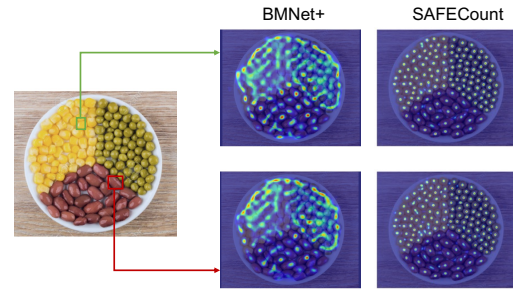


Figure 1. Visualizations of the density maps predicted by two recently proposed class-agnostic counting methods, *i.e.*, BMNet+[32] and SAFECOUNT [41]. They fail to count the objects of interest when multiple objects of different classes appear in the same image.

a similarity-aware feature enhancement framework to better capture the support-query relationship. These methods perform quite well on the current benchmark, *i.e.* FSC-147, in which images only contain objects from a single dominant class. However, we observe that when objects of multiple classes appear in the same image, these methods tend to greedily count every single object regardless of the exemplars (see Figure 1). This issue greatly limits the potential applicability of these methods in real-world scenarios. A possible reason is that the current counting datasets only contain single-class training images, causing the counting models to overlook the inter-class discriminability due to the absence of multi-class training data.

A natural solution to resolve this issue is to train the counting model with images containing objects of multiple classes. However, building such labeled multi-class datasets for counting is not an easy task: it is non-trivial to collect images for counting with a large diversity of categories, and annotating them is costly since point annotation is required for instances from different classes. An alternative way is to synthesize multi-class training data from single-class images. By simply concatenating two or more images of different classes, we can easily create a large amount of multi-class data without additional annotation costs. However, our experiments show that while the model trained on

these images indeed performs better on multi-class test images, the performance on single-class counting drops significantly (5.1). This could be because, in order for the model to selectively count the objects of interest, it needs to recognize certain discriminative features that can distinguish between different classes. This will inevitably sacrifice some of its robustness against the variations within the same class. In other words, there is a trade-off between invariance and discriminative power for the counting model [34].

Due to this trade-off, instead of training an end-to-end model for multi-class counting, our strategy is to localize the area containing the objects of interest first and then count the objects inside. Given a multi-class image for counting and a few exemplars, our goal is to obtain a segmentation mask highlighting the regions of interest. Such an exemplar-based segmentation model can be easily trained if mask annotations are available. However, this is not the case for the current counting datasets [30, 17], and collecting such annotations is time-consuming and labor-intensive. To this end, we propose a method to obtain pseudo segmentation masks using only box exemplars and dot annotations. We show that a segmentation model trained with only these pseudo-labeled masks can effectively localize objects of interest for multi-class counting.

We aim to obtain a mask covering all the objects that belong to the same class as the exemplars while not including any irrelevant object or background. We show that an unsupervised clustering method, K -Means, can be used for this purpose. In particular, given a synthetic multi-class image, a few annotated exemplars, and a pre-trained single-class counting model, we first represent each mask pixel with an image patch based on the receptive field of the network. Then we extract the feature embeddings for all the image patches as well as the provided exemplars and run K -Means clustering on them. We consider the patches whose embeddings fall into the same cluster as the exemplar to contain the objects of interest and assign positive labels to the corresponding mask pixels. We assign negative labels otherwise. Note that the output of K -Means is sensitive to the choice of K , which is hard to determine for each image. In our case, we choose the K that results in a pseudo mask that best benefits the pre-trained counting model, *i.e.*, the counting model can produce the density map closest to the ground truth map after the pseudo mask is applied. The obtained pseudo masks can then be used as the supervision signal to train an exemplar-based segmentation model.

To evaluate the performance of different methods on multi-class counting, we introduce two new benchmarks, a synthetic multi-class dataset originating from FSC-147, and a new test set of real images in which objects from multiple classes are present. Our proposed method outperforms current counting methods by a large margin on these two benchmarks.

In short, our main contributions are:

- We identify a critical issue of the previous class-agnostic counting methods, *i.e.*, greedily counting every object when objects of multiple classes appear in the same image, and propose a simple segment-and-count strategy to resolve it.
- We propose a method to obtain pseudo-labeled segmentation masks using only annotated exemplars and use them to train a segmentation model.
- We introduce two benchmarks for multi-class counting, on which our proposed method outperforms the previous counting methods by a large margin.

2. Related Work

2.1. Class-specific Object Counting

Class-specific object counting aims to count objects from pre-defined categories, such as humans [22, 46, 43, 37, 33, 19, 1, 44, 31, 45, 39, 24, 35], animals [3], cells [38] and cars [27, 17]. Generally, there are two groups of class-specific counting methods: detection-based methods [6, 17, 21] and regression-based methods [44, 9, 10, 36, 46, 5, 25]. Detection-based methods apply an object detector on the image and count the number of objects based on the detected boxes. However, detection-based methods often struggle with detecting tiny objects. Regression-based methods predict a density map for each input image, and the final result is obtained by summing up the pixel values. Both types of methods require a large amount of training data with rich training annotations. Moreover, they can not be used to count objects of arbitrary categories at test time.

2.2. Class-agnostic Object Counting

Class-agnostic object counting aims to count arbitrary categories given only a few exemplars [26, 30, 40, 32, 14, 28, 23, 42, 2]. Previous methods mostly focus on how to better capture the similarity between exemplars and image features. For example, SAFECOUNT [41] uses a similarity-aware feature enhancement framework to better model the support-query relationship. RCAC [14] is proposed to enhance the counter’s robustness against intra-class diversity. Nguyen *et al.* [28] recently introduce new benchmarks for object counting, which contains images of objects from multiple classes, originating from the FSC-147 and LVIS [15] datasets. However, these benchmarks are designed for the task of jointly detecting and counting object instances in complex scenes, where the central focus is on how to detect them accurately.

2.3. Unsupervised Semantic Segmentation

A closely related task to ours is unsupervised semantic segmentation [20, 8, 29, 7, 16, 18, 12, 13], which aims

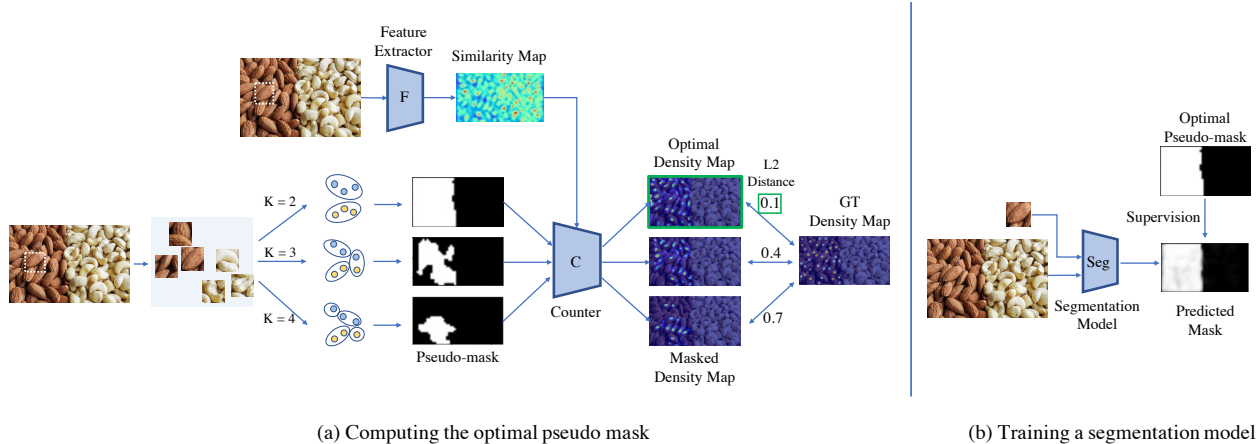


Figure 2. Overview of our approach. We propose a method to obtain the pseudo segmentation masks using only box exemplars and dot annotations (a), and then use the obtained pseudo masks to train an exemplar-based segmentation model (b). Specifically, given a multi-class image and a few annotated exemplars, we crop a set of image patches, each of which corresponds to a mask pixel (we only visualize 6 patches here for simplicity). We run K -Means clustering on the feature embeddings extracted from all cropped patches and the exemplars. Those pixels whose embeddings fall into the same cluster as the exemplar form an object mask indicating the image area containing the objects of interest. We find the optimal number of clusters, K , such that the counting model can produce the density map closest to the ground truth after the pseudo mask is applied. We use the obtained pseudo masks to train an exemplar-based segmentation model, which can then be used to infer the object mask given an arbitrary test image.

to discover classes of objects within images without external supervision. IIC [20] attempts to learn semantically meaningful features through transformation equivariance. PiCIE [8] further improves on IIC’s segmentation results by incorporating geometric consistency as an inductive bias. Although these methods can semantically segment images without supervision, they typically require a large-scale dataset [4, 11] to learn an embedding space that is cluster-friendly. Moreover, the label space of semantic segmentation is limited to a set of pre-defined categories. In comparison, our goal is to localize the region of interest specified by a few exemplars, which can belong to an arbitrary class.

3. Method

In order to perform multi-class object counting, our strategy is to compute a mask that can be applied to the similarity maps of a pre-trained counting model to localize the area containing the objects of interest and count the objects inside. Figure 2 summarizes our approach. We propose a method to obtain pseudo segmentation masks using only box exemplars and dot annotations, and then use these pseudo masks to train an exemplar-based segmentation model. Specifically, given a multi-class image and a few annotated exemplars, we tile the input image into different patches, each of which corresponds to a pixel on the mask. We run K -Means clustering on the feature embeddings extracted from all cropped patches and the exemplars. Those mask pixels whose corresponding patch embeddings fall into the same cluster as the exemplar will form an ob-

ject mask indicating the image area containing the objects of interest. We find the optimal number of clusters, K , such that a pre-trained single-class counting model can produce the density map closest to the ground truth after the pseudo mask is applied. We use the obtained pseudo masks to train an exemplar-based segmentation model, which can then be used to infer the object mask given an arbitrary test image. For the rest of the paper, we denote the pre-trained single-class counting model as the “base counting model”. Below we will first describe how we train this base counting model and then present the detail of our proposed multi-class counting method.

3.1. Training The Base Counting Model

We first train a base counting model using images from the single-class counting dataset [30]. Similar to previous works [30, 32], the base counting model uses the input image and the exemplars to obtain a density map for object counting. The model consists of a feature extractor F and a counter C . Given a query image I and an exemplar B of an arbitrary class c , we input I and B to the feature extractor to obtain the corresponding output, denoted as $F(I)$ and $F(B)$ respectively. $F(I)$ is a feature map of size $d * h_I * w_I$ and $F(B)$ is a feature map of size $d * h_B * w_B$. We further perform global average pooling on $F(B)$ to form a feature vector b of d dimensions.

After this feature extraction step, we obtain the similarity map S by correlating the exemplar feature vector b with the image feature map $F(I)$. Specifically, let $w_{(i,j)} = F_{(i,j)}(I)$ be the channel feature at spatial position (i, j) , S can be

computed by:

$$S_{(i,j)}(I, B) = w_{(i,j)}^T b. \quad (1)$$

In the case where n exemplars are given, we use Eq. 1 to calculate n similarity maps, and the final similarity map is the average of these n similarity maps.

We then concatenate the image feature map $F(I)$ with the similarity map S , and input them into the counter C to predict a density map D . The final predicted count N is obtained by summing over the predicted density map D :

$$N = \sum_{i,j} D_{(i,j)}, \quad (2)$$

where $D_{(i,j)}$ denotes the density value for pixel (i, j) . The supervision signal for training the counting model is the L_2 loss between the predicted density map and the ground truth density map:

$$L_{\text{count}} = \|D(I, B) - D^*(I, B)\|_2^2, \quad (3)$$

where D^* denotes the ground truth density map.

3.2. Multi-class Object Counting

3.2.1 Pseudo-Labeling Segmentation Masks

In this section, we describe our method to obtain pseudo-masks using only box exemplars and dot annotations. The mask is of the same size as the similarity map from the base counting model and each pixel on the mask is associated with a region in the original image. Ideally, the pixel value on the mask is 1 if the corresponding region contains the object of interest and 0 elsewhere. Specifically, for the pixel from the mask M at location (i, j) , we find its corresponding patch $p(i, j)$ in the input image centering around (i_I, j_I) , where $i_I = i * r + 0.5 * r$ and $j_I = j * r + 0.5 * r$. Here, r is the downsampling ratio between the original image and the similarity map. The width and height of $p(i, j)$ are set to be the mean of the width and height of the exemplar boxes.

We denote $\mathbb{P} = \{p_1, p_2, \dots, p_n\}$ as a set of image patches, each of which corresponds to one pixel in the mask. The goal is to assign a binary label to each patch indicating if it contains the object of interest or not. To achieve this, we first extract the ImageNet features for all patches in \mathbb{P} to get a set of embeddings $\mathbb{F} = \{f_1, f_2, \dots, f_n\}$. Then we compute the average of the embeddings extracted from the exemplar boxes in this image, denoted as f_B . We run K -means on the union of $\{f_1, f_2, \dots, f_n\}$ and $\{f_B\}$. Those patches whose embeddings fall into the same cluster as f_B will be considered to contain the object of interest, and result in a 1 value in the corresponding pixel of the mask. On the contrary, the pixel value will be 0 if the corresponding patch embedding falls into a different cluster as f_B . Here K -Means groups

similar objects together, which can serve our purpose of segmenting objects belonging to different classes.

It is worth noting that the number of clusters, denoted as K , has a large effect on the output binary mask and the final counting results. If K is too small, too many patch embeddings will fall into the same cluster as the exemplar embedding and the counter will over-count the objects; if K is set too high, too few embeddings will fall into the same cluster, which results in too many regions being masked out. In our case, we find the optimal K for each image in the multi-class training set that results in the binary mask that minimizes the counting error. Specifically, given a multi-class image \bar{I} and an exemplar \bar{B} , let $S(\bar{I}, \bar{B})$ denote the similarity map outputted by the pre-trained counting model, and $M(\bar{I}, \bar{B})^k$ denote the mask obtained when the number of clusters is set to k . By applying $M(\bar{I}, \bar{B})^k$ on $S(\bar{I}, \bar{B})$, the similarity scores on the non-target area are set to a small constant value ϵ and the similarity scores on the target area remain the same:

$$S(\bar{I}, \bar{B})_{(i,j)}^k = \begin{cases} S(\bar{I}, \bar{B})_{(i,j)}, & \text{if } M(\bar{I}, \bar{B})_{(i,j)}^k = 1, \\ \epsilon, & \text{otherwise.} \end{cases} \quad (4)$$

We then input $S(\bar{I}, \bar{B})^k$ to the pre-trained counter C to get the corresponding density map $D(\bar{I}, \bar{B})^k$. We find the optimal k such that the L_2 loss between the predicted density map and the ground truth density map is the smallest:

$$k^* = \underset{k}{\operatorname{argmin}} \|D(\bar{I}, \bar{B})^k - D^*(\bar{I})\|_2^2, \quad (5)$$

where k^* denotes the optimal k and $D^*(\bar{I})$ denotes the ground truth density map for input image \bar{I} .

3.2.2 Training Exemplar-based Segmentation Model

After obtaining the optimal masks for all the images in the multi-class training set, we train a segmentation model P to predict the pseudo segmentation masks based on the input image and the corresponding exemplar. In particular, suppose we have a multi-class image \bar{I} and an exemplar \bar{B} , we first input \bar{I} and \bar{B} to the segmentation model to get the corresponding feature map output $P(\bar{I})$ and $P(\bar{B})$. We then apply global average pooling on $P(\bar{B})$ to form a feature vector v . In the case where multiple exemplars are provided, we apply global average pooling on each $P(\bar{B})$ and the final vector v is the average of all these pooling vectors.

The predicted mask M^P is obtained by computing the cosine similarity between v and the channel feature at each spatial location of $P(\bar{I})$. Specifically, the value of the predicted mask at position (i, j) is:

$$M_{(i,j)}^P(\bar{I}, \bar{B}) = \cos(P_{(i,j)}(\bar{I})^T, v). \quad (6)$$

The supervision signal for training this segmentation model is the L_2 loss between the predicted mask and the optimal mask obtained by finding the best k with Eq. 5:

$$L_{\text{seg}} = \|M^p(\bar{I}, \bar{B}) - M^*(\bar{I}, \bar{B})\|_2^2, \quad (7)$$

where $M^*(\bar{I}, \bar{B})$ denotes the optimal mask under k^* .

3.2.3 Inference on Multi-class Testing Data

After the exemplar-based segmentation model is trained, we use it together with the pre-trained counting model to perform multi-class object counting. Given an input image for testing, we first input it to the feature extractor of the pre-trained counting model to get the corresponding similarity map. Then we use the segmentation model to predict a coarse mask where high values indicate the region of interests. We binarize this predicted mask with a simple threshold and apply it on the similarity map based on Eq. 4. The counter then take the masked similarity map as input and predict the density map and final object counts.

4. Experiments

4.1. Implementation Details

Network architecture For the base counting model, we use ResNet-50 as the backbone of the feature extractor, initialized with weights of a pre-trained ImageNet model. The backbone outputs feature maps of 1024 channels. For each query image, the number of channels is reduced to 256 using 1×1 convolution. For each exemplar, the feature maps are first processed with global average pooling and then linearly mapped to a 256-d feature vector. The counter consists of 5 convolution and bilinear upsampling layers to regress a density map of the same size as the query image. The segmentation model shares the same architecture as the backbone of the feature extractor. The output mask is of the same size as the similarity map from the base counting model.

Dataset We train the base counting model on the FSC-147 dataset. FSC-147 is the first large-scale dataset for class-agnostic counting. It includes 6135 images from 147 categories varying from animals, kitchen utensils, to vehicles. The categories in training, validation, and test sets have no overlap. We create synthetic multi-class images from FSC-147 dataset to train the segmentation model. Specifically, we randomly select two images belonging to different classes, crop a part from each image and then concatenate the two cropped parts horizontally. To evaluate the performance of multi-class counting on real images, we further collect a test set of 450 multi-class images. For each image in this test set, there are at least two categories whose object instances appear multiple times. We provide dot annotations for 600 groups of object instances. The synthetic validation set and test set contain 1431 and 1359 images

respectively. We test the trained model on both the synthetic multi-class images and our collected real multi-class images.

Training details Both the base counting model and the segmentation model are trained using the AdamW optimizer with a fixed learning rate of 10^{-5} and a batch size of 8. The base counting model is trained for 300 epochs and the segmentation model is trained for 20 epochs. We resize the input query image to a fixed height of 384, and the width is adjusted accordingly to preserve the aspect ratio of the original image. Exemplars are resized to 128×128 before being fed into the feature extractor. We run K -means on the extracted patch embeddings to find the K that leads to the optimal mask for each image. The embeddings are extracted from a pre-trained ImageNet backbone. The threshold for binarizing the segmentation mask is 0.6 and the number of clusters K ranges from 2 to 6.

4.2. Evaluation Metrics

For our collected multi-class test set, the counting error ϵ for image i is defined as $\epsilon_i = |y_i - \hat{y}_i|$, where y_i and \hat{y}_i are the ground truth and the predicted number of objects respectively. For our synthetic multi-class test set, the objects of interest are only present in the left / right-half part of the image. Ideally, the predicted number of objects should be close to the ground truth in the area of interest while being zero elsewhere. Thus, we define the counting error as $\epsilon_i = |y_i - \hat{y}_i| + \tilde{y}_i$, where \hat{y}_i and \tilde{y}_i denote the predicted number of objects in the interest area and non-interest area respectively.

We use Mean Average Error (MAE), Root Mean Squared Error (RMSE), Normalized Relative Error (NAE) and Squared Relative Error (SRE) to measure the performance of different object counters over all testing images. In particular, $\text{MAE} = \frac{1}{n} \sum_{i=1}^n \epsilon_i$; $\text{RMSE} = \sqrt{\frac{1}{n} \sum_{i=1}^n \epsilon_i^2}$; $\text{NAE} = \frac{1}{n} \sum_{i=1}^n \frac{\epsilon_i}{y_i}$; $\text{SRE} = \sqrt{\frac{1}{n} \sum_{i=1}^n \frac{\epsilon_i^2}{y_i^2}}$ where n is the number of testing images.

4.3. Comparing Methods

We compare our method with recent class-agnostic counting methods, including CounTR (Counting TRansformer [23]), FamNet (Few-shot adaptation and matching Network [30]), SAFECOUNT (Similarity-Aware Feature Enhancement block for object Counting [41]) and BMNet (Bilinear Matching Network [32]).

4.4. Results

Quantitative results. Table 1 compares our proposed method with previous class-agnostic counting methods on our synthetic multi-class validation and test sets. (We include the results on single-class datasets in the Supp. Mat due to space limitations). The performance of all these

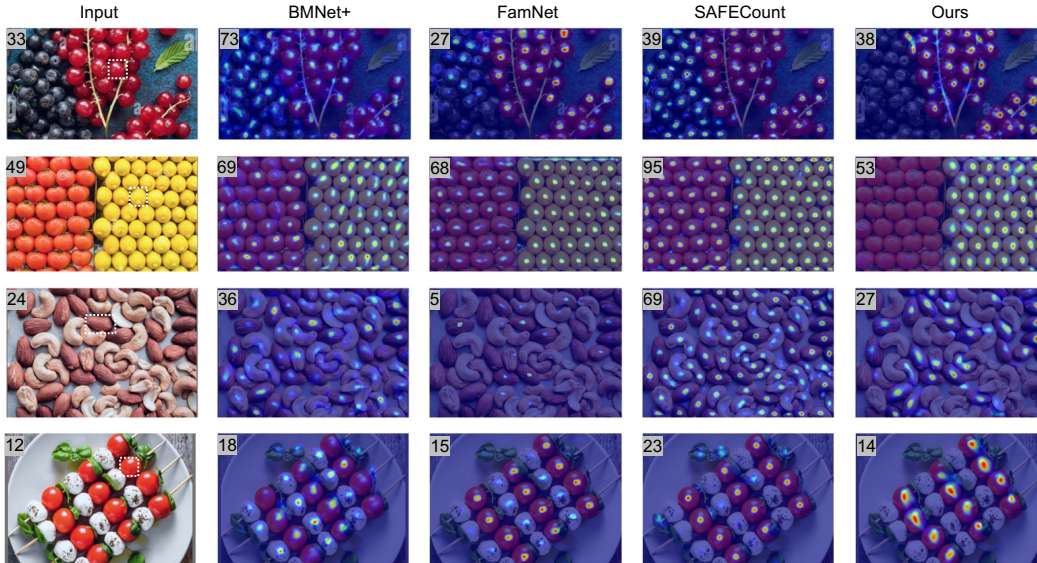


Figure 3. Qualitative results on our collected multi-class counting test dataset. We visualize a few input images, the corresponding annotated exemplar (bounded in a dashed white box) and the predicted density maps. Predicted object counts are shown at the top-left corner. Our predicted density maps can highlight the objects of interest specified by the annotated box, which will lead to more accurate object counts.

Method	Val Set				Test Set			
	MAE	RMSE	NAE	SRE	MAE	RMSE	NAE	SRE
CountTR [41]	32.29	47.07	1.89	3.31	40.20	83.03	1.85	3.79
FamNet [30]	18.15	33.16	0.63	4.42	22.22	40.85	0.79	9.29
FamNet+ [30]	27.74	39.78	1.33	7.29	29.90	43.59	1.16	8.82
BMNet [32]	32.39	46.01	1.75	9.86	36.94	46.73	1.65	9.46
BMNet+ [32]	31.09	42.43	1.75	9.51	39.78	57.85	1.81	11.96
SAFECount [41]	22.58	34.68	1.21	2.18	26.44	40.68	1.14	2.89
Ours	14.34	26.03	0.61	4.48	11.13	16.96	0.41	2.80

Table 1. Quantitative comparisons on our synthetic multi-class dataset. Our proposed method outperforms the previous class-agnostic counting methods by a large margin, achieving the lowest mean average error on both validation and test set.

Method	MAE	RMSE	NAE	SRE
CountTR [41]	24.73	45.16	1.62	3.10
FamNet [30]	13.54	21.22	0.65	3.38
FamNet+ [30]	19.42	38.46	0.95	6.13
BMNet [32]	21.92	37.09	1.18	1.68
BMNet+ [32]	25.55	40.35	1.36	1.81
SAFECount [41]	23.57	40.99	1.25	1.69
Ours	6.97	13.03	0.37	0.54

Table 2. Quantitative comparisons on our collected multi-class dataset. Our proposed method has the lowest counting error compared with the previous class-agnostic counting methods.

methods drops significantly when tested on our synthetic dataset. The state-of-the-art single-class counting method CountTR [23], for example, shows a 20.34 error increase w.r.t. validation MAE (from 13.13 to 32.29) and a 28.25 error increase w.r.t. test MAE (from 11.95 to 40.20). Interestingly, we find that FamNet, which has the largest counting error on the single-class test set among these methods, performs best on our synthetic multi-class dataset. Unlike other methods, FamNet keeps the backbone of the counting model fixed without any adaptation, which prevents

the model from over-capturing the intra-class similarity and greedily counting everything. This further validates that there is a trade-off between single-class and multi-class counting performance. Our proposed method outperforms the other methods by a large margin, achieving 14.34 on validation MAE and 11.13 on test MAE.

Table 2 shows the comparison with previous methods on our collected test set. Similarly, our proposed method significantly outperforms other methods by a large margin, as reflected by a reduction of 6.82 w.r.t. MAE over FamNet and 14.77 w.r.t. MAE over BMNet.

Qualitative analysis. In Figure 3, we present a few input testing images, the corresponding annotated bounding box and the density maps produced by different counting methods. We can see that when there are objects of multiple classes present in the image, previous methods fail to distinguish them accurately, which often leads to over-counting. In comparison, the density map predicted by our method can highlight the objects of interest specified by the annotated box, even for the hard case where the objects are

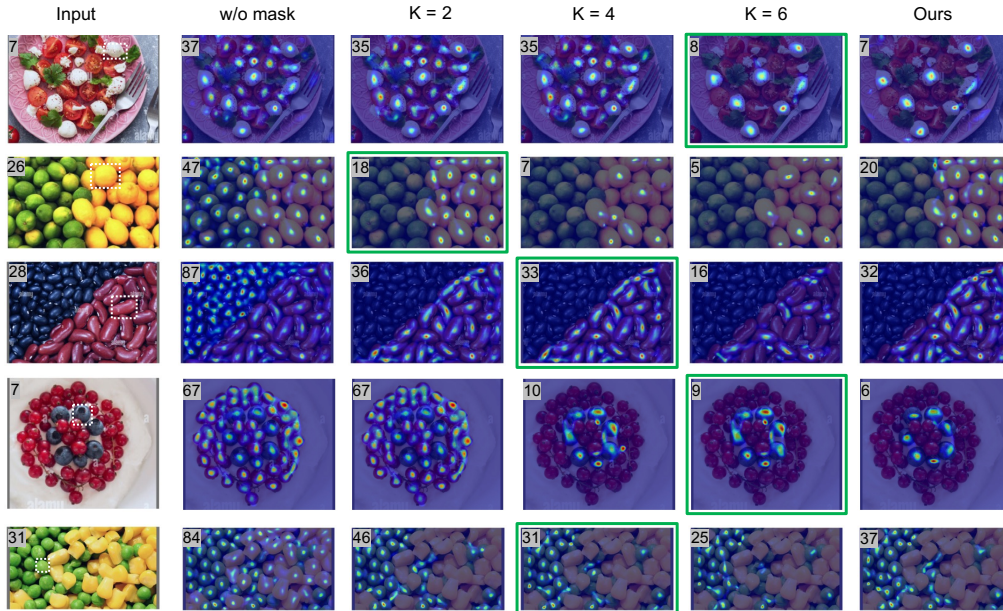


Figure 4. Qualitative analysis on the number of clusters. We visualize a few input images, the corresponding annotated exemplar (bounded in a dashed white box) and the density maps when using masks computed from K -means as well as predicted by our segmentation model. Predicted counting results are shown at the top-left corner. The density maps under the optimal K are framed in green. The value of K has a large effect on the counting results and the optimal K varies from image to image.

irregularly placed in the image (the 3rd row).

K	2	3	4	5	6	Ours
MAE	15.13	10.77	8.17	7.98	8.03	6.97
RMSE	28.09	20.71	15.38	14.93	15.31	13.03
NAE	0.94	0.63	0.44	0.42	0.40	0.37
SRE	1.68	1.18	0.69	0.62	0.54	0.54

Table 3. Quantitative analysis on the number of clusters. Our proposed method outperforms K -Means under different values of K on our collected multi-class test set.

5. Analyses

5.1. Comparison with Training with Synthetic Data

Our strategy for multi-class counting is to compute a coarse mask to localize the image area of interest first and then count the objects inside with a single-class counting model. An alternative way is to train an end-to-end model for multi-class counting using images containing objects from multiple classes. In this section, we compare the performance of these two strategies. Specifically, we use our synthetic multi-class images to fine-tune three pre-trained single-class counting models: BMNet+ [32], FamNet+ [30] and SAFECount [41]. Results are summarized in Table 4. As shown in the table, after fine-tuning on multi-class images, although the counting error on the multi-class test set is reduced, the performance on the single-class test set drops significantly for all three counting methods. Our method, in comparison, achieves the best performance for multi-class

counting without sacrificing the performance on the single-class test set.

5.2. Analysis on the Number of Clusters

When running K -means, the number of clusters, K , has a large effect on the computed binary mask and the final counting results. However, it is non-trivial to determine K given an arbitrary image. To resolve this issue, we first compute the optimal pseudo masks for the training images based on the dot annotations. Then we train an exemplar-based segmentation model to predict the obtained pseudo masks. During testing, we can use the trained model to predict the segmentation mask based on exemplars. In this section, we provide analyses on how K affects the final counting results and show a comparison with our proposed method.

5.2.1 Quantitative Results

We report the counting performance when computing masks by running K -means under different values of K as well as using our predicted masks on the collected multi-class test set. Results are summarized in Table 3. As K goes from 2 to 6, both the MAE and RMSE decrease first and then increase, achieving the lowest when $K = 5$, *i.e.*, 7.98 w.r.t. MAE and 14.93 w.r.t. RMSE. Using our predicted masks outperforms the performance under the best K by 12.6% w.r.t. MAE and 12.7% w.r.t. RMSE, which demonstrates the advantages of using our trained segmentation model to predict the mask.

Method	Training Set	Multi Set		Single Set			
		Test MAE	Test RMSE	Val MAE	Val RMSE	Test MAE	Test RMSE
BMNet+	Single	25.55	40.35	15.74	58.53	14.62	91.83
	Single+Syn-multi	11.44	23.22	24.24	73.42	20.89	99.04
FamNet+ [30]	Single	19.42	39.78	23.75	69.07	22.08	99.54
	Single+Syn-multi	11.31	18.84	29.45	94.33	26.93	116.12
SAFECount [30]	Single	23.57	40.99	14.42	51.72	13.56	91.30
	Single+Syn-multi	9.80	32.40	27.65	58.01	27.24	100.55
Ours	Single+Syn-multi	6.97	13.03	18.55	61.12	20.68	109.14

Table 4. Comparison with training other class-agnostic counting methods (BMNet+, FamNet+ and SAFECount) using our synthetic multi-class images. Although the counting error on the multi-class test set is reduced, the performance on the single-class test set drops significantly for all three baseline methods.

5.2.2 Qualitative Results

In Figure 4, we visualize a few input images and the corresponding density maps when using masks computed from K -means as well as using masks predicted by our segmentation model. As can be seen from the figure, the choice of K has a large effect on the counting results. If K is too small, too many patch embeddings will fall into the same cluster as the exemplar embedding and the counter will over-count the objects (the 4th row when $K = 2$); if K is too large, too few embeddings will fall into the same cluster, which results in too many regions being masked out (the 2nd row when $K = 6$). The optimal K varies from image to image, and it is non-trivial to determine the optimal K for an arbitrary image. Using our trained segmentation model, on the other hand, does not require any prior knowledge about the test image while producing more accurate masks and density maps based on the provided exemplars.

5.3. Analysis on the Trade-off between Invariance and Discriminative Power

We observe that there is a trade-off between single-class and multi-class counting performance. Our explanation is that when images contain objects from a single dominant class, the model will focus only on capturing the intra-class similarity while ignoring the inter-class discrepancy; when objects from multiple classes exist in the image, the model will focus more on the inter-class discrepancy in order to distinguish between them. To get a better understanding of this trade-off, we provide the detailed feature distribution statistics in Table 5. Specifically, we measure the intra-class distance and inter-class distance of the exemplar features extracted from our baseline counting model before and after fine-tuning using the synthetic multi-class dataset. Intra-class distance refers to the mean of Euclidean distance between a feature embedding and the corresponding class’s embedding center. Inter-class distance refers to the mean of the minimum distance between embedding centers. As shown in the table, after fine-tuning the model using the synthetic multi-class dataset, both intra-class distance and inter-class distance increase. Larger inter-class

distance means features from different classes are more separable, suggesting a better discriminative power of the model; larger intra-class distance means features within the same class are less compact, suggesting inferior robustness against within-class variations of the model. This trade-off between invariance and discriminative power makes it non-trivial to train one model to perform well on single-class counting and multi-class counting simultaneously.

Split	Training Set	Intra	Inter	Single	Syn-multi
				MAE	MAE
Val	Single	2.35	1.12	18.55	32.46
	Single+Syn-multi	2.90	1.30	32.36	25.74
Test	Single	2.31	1.19	20.68	42.22
	Single+Syn-multi	2.86	1.48	32.34	29.12

Table 5. Analysis on the trade-off between invariance and discriminative power of the counting model. After fine-tuning on our synthetic multi-class dataset, both the intra-class and inter-class distances of exemplar features become larger.

6. Conclusion

In this paper, we identify a critical issue of the previous class-agnostic counting methods, *i.e.*, greedily counting every object when objects of multiple classes appear in the same image. We show that simply training the counting model with multi-class data can alleviate this issue but often at the price of sacrificing the ability to count objects from a single class accurately. Thus, our strategy is to localize the area of interest first and then count the objects inside the area. To do this, we propose a method to obtain pseudo segmentation masks using only box exemplars and dot annotations. We show that a segmentation model trained with these pseudo-labeled masks can effectively localize the image area containing the objects of interest for an arbitrary multi-class image. We further introduce two new benchmarks to evaluate the performance of different methods on multi-class counting, on which our method outperforms the other methods by a significant margin.

References

- [1] Shahira Aousamra, Minh Hoai, Dimitris Samaras, and Chao Chen. Localization in the crowd with topological constraints. *ArXiv*, abs/2012.12482, 2021.
- [2] Carlos Arteta, Victor S. Lempitsky, Julia Alison Noble, and Andrew Zisserman. Interactive object counting. In *ECCV*, 2014.
- [3] Carlos Arteta, Victor S. Lempitsky, and Andrew Zisserman. Counting in the wild. In *ECCV*, 2016.
- [4] Holger Caesar, Jasper R. R. Uijlings, and Vittorio Ferrari. Coco-stuff: Thing and stuff classes in context. *2018 IEEE/CVF Conference on Computer Vision and Pattern Recognition*, pages 1209–1218, 2016.
- [5] Antoni B. Chan, Zhang-Sheng John Liang, and Nuno Vasconcelos. Privacy preserving crowd monitoring: Counting people without people models or tracking. *2008 IEEE Conference on Computer Vision and Pattern Recognition*, pages 1–7, 2008.
- [6] Prithvijit Chattopadhyay, Ramakrishna Vedantam, Ramprasaath R. Selvaraju, Dhruv Batra, and Devi Parikh. Counting everyday objects in everyday scenes. *2017 IEEE Conference on Computer Vision and Pattern Recognition (CVPR)*, pages 4428–4437, 2017.
- [7] Mickaël Chen, Thierry Artières, and Ludovic Denoyer. Unsupervised object segmentation by redrawing. In *Neural Information Processing Systems*, 2019.
- [8] Jang Hyun Cho, Utkarsh Mall, Kavita Bala, and Bharath Hariharan. Picie: Unsupervised semantic segmentation using invariance and equivariance in clustering. *2021 IEEE/CVF Conference on Computer Vision and Pattern Recognition (CVPR)*, pages 16789–16799, 2021.
- [9] Hisham Cholakkal, Guolei Sun, Fahad Shahbaz Khan, and Ling Shao. Object counting and instance segmentation with image-level supervision. *2019 IEEE/CVF Conference on Computer Vision and Pattern Recognition (CVPR)*, pages 12389–12397, 2019.
- [10] Hisham Cholakkal, Guolei Sun, Salman Hameed Khan, Fahad Shahbaz Khan, Ling Shao, and Luc Van Gool. Towards partial supervision for generic object counting in natural scenes. *IEEE Transactions on Pattern Analysis and Machine Intelligence*, 44:1604–1622, 2022.
- [11] Marius Cordts, Mohamed Omran, Sebastian Ramos, Timo Rehfeld, Markus Enzweiler, Rodrigo Benenson, Uwe Franke, Stefan Roth, and Bernt Schiele. The cityscapes dataset for semantic urban scene understanding. *2016 IEEE Conference on Computer Vision and Pattern Recognition (CVPR)*, pages 3213–3223, 2016.
- [12] Wouter Van Gansbeke, Simon Vandenhende, Stamatios Georgoulis, and Luc Van Gool. Unsupervised semantic segmentation by contrasting object mask proposals. *2021 IEEE/CVF International Conference on Computer Vision (ICCV)*, pages 10032–10042, 2021.
- [13] Wouter Van Gansbeke, Simon Vandenhende, Stamatios Georgoulis, Marc Proesmans, and Luc Van Gool. Scan: Learning to classify images without labels. In *European Conference on Computer Vision*, 2020.
- [14] Shenjian Gong, Shanshan Zhang, Jian Yang, Dengxin Dai, and Bernt Schiele. Class-agnostic object counting robust to intraclass diversity. *2022 European Conference on Computer Vision (ECCV)*, 2022.
- [15] Agrim Gupta, Piotr Dollár, and Ross B. Girshick. Lvis: A dataset for large vocabulary instance segmentation. *2019 IEEE/CVF Conference on Computer Vision and Pattern Recognition (CVPR)*, pages 5351–5359, 2019.
- [16] Mark Hamilton, Zhoutong Zhang, Bharath Hariharan, Noah Snavely, and William T. Freeman. Unsupervised semantic segmentation by distilling feature correspondences. *Proceedings of the International Conference on Learning Representations (ICLR)*, 2022.
- [17] Meng-Ru Hsieh, Yen-Liang Lin, and Winston H. Hsu. Drone-based object counting by spatially regularized regional proposal network. *2017 IEEE International Conference on Computer Vision (ICCV)*, pages 4165–4173, 2017.
- [18] Jyh-Jing Hwang, Stella X. Yu, Jianbo Shi, Maxwell D. Collins, Tien-Ju Yang, Xiao Zhang, and Liang-Chieh Chen. Segsort: Segmentation by discriminative sorting of segments. *2019 IEEE/CVF International Conference on Computer Vision (ICCV)*, pages 7333–7343, 2019.
- [19] Haroon Idrees, Muhammad Tayyab, Kishan Athrey, Dong Zhang, Somaya Ali Al-Maadeed, Nasir M. Rajpoot, and Mubarak Shah. Composition loss for counting, density map estimation and localization in dense crowds. In *ECCV*, 2018.
- [20] Xu Ji. Invariant information clustering for unsupervised image classification and segmentation. 2019.
- [21] Issam H. Laradji, Negar Rostamzadeh, Pedro H. O. Pinheiro, David Vázquez, and Mark W. Schmidt. Where are the blobs: Counting by localization with point supervision. *ArXiv*, abs/1807.09856, 2018.
- [22] Dongze Lian, Jing Li, Jia Zheng, Weixin Luo, and Shenghua Gao. Density map regression guided detection network for rgb-d crowd counting and localization. *2019 IEEE/CVF Conference on Computer Vision and Pattern Recognition (CVPR)*, pages 1821–1830, 2019.
- [23] Chang Liu, Yujie Zhong, Andrew Zisserman, and Weidi Xie. Countr: Transformer-based generalised visual counting. 2022.
- [24] Weizhe Liu, N. Durasov, and P. Fua. Leveraging self-supervision for cross-domain crowd counting. *2022 IEEE/CVF Conference on Computer Vision and Pattern Recognition (CVPR)*, pages 5331–5342, 2022.
- [25] Weizhe Liu, Mathieu Salzmann, and Pascal V. Fua. Context-aware crowd counting. *2019 IEEE/CVF Conference on Computer Vision and Pattern Recognition (CVPR)*, pages 5094–5103, 2019.
- [26] Erika Lu, Weidi Xie, and Andrew Zisserman. Class-agnostic counting. In *ACCV*, 2018.
- [27] Terrell N. Mundhenk, Goran Konjevod, Wesam A. Sakla, and Kofi Boakye. A large contextual dataset for classification, detection and counting of cars with deep learning. In *ECCV*, 2016.
- [28] Thanh Nguyen, Chau Pham, Khoi Nguyen, and Minh Hoai. Few-shot object counting and detection. *2022 European Conference on Computer Vision (ECCV)*, 2022.

- [29] Yassine Ouali, Céline Hudelot, and Myriam Tami. Autoregressive unsupervised image segmentation. *2020 European Conference on Computer Vision (ECCV)*, 2020.
- [30] Viresh Ranjan, Udbhav Sharma, Thua Nguyen, and Minh Hoai. Learning to count everything. *2021 IEEE/CVF Conference on Computer Vision and Pattern Recognition (CVPR)*, pages 3393–3402, 2021.
- [31] Deepak Babu Sam, Abhinav Agarwalla, Jimmy Joseph, Vishwanath A. Sindagi, R. Venkatesh Babu, and Vishal M. Patel. Completely self-supervised crowd counting via distribution matching. *2022 European Conference on Computer Vision (ECCV)*, 2022.
- [32] Min Shi, Hao Lu, Chen Feng, Chengxin Liu, and Zhiguo Cao. Represent, compare, and learn: A similarity-aware framework for class-agnostic counting. *2021 IEEE/CVF Conference on Computer Vision and Pattern Recognition (CVPR)*, 2022.
- [33] Vishwanath A. Sindagi, Rajeev Yasarla, and Vishal M. Patel. Pushing the frontiers of unconstrained crowd counting: New dataset and benchmark method. *2019 IEEE/CVF International Conference on Computer Vision (ICCV)*, pages 1221–1231, 2019.
- [34] Manik Varma and Debajyoti Ray. Learning the discriminative power-invariance trade-off. *2007 IEEE 11th International Conference on Computer Vision*, pages 1–8, 2007.
- [35] Jia Wan, Ziquan Liu, and Antoni B. Chan. A generalized loss function for crowd counting and localization. *2021 IEEE/CVF Conference on Computer Vision and Pattern Recognition (CVPR)*, pages 1974–1983, 2021.
- [36] Boyu Wang, Huidong Liu and Dimitris Samaras, and Minh Hoai Nguyen. Distribution matching for crowd counting. In *NeurIPS*, 2020.
- [37] Qi Wang, Junyu Gao, Wei Lin, and Xuelong Li. Nwpu-crowd: A large-scale benchmark for crowd counting and localization. *IEEE Transactions on Pattern Analysis and Machine Intelligence*, 43:2141–2149, 2021.
- [38] Weidi Xie, J. Alison Noble, and Andrew Zisserman. Microscopy cell counting and detection with fully convolutional regression networks. *Computer Methods in Biomechanics and Biomedical Engineering: Imaging & Visualization*, 6:283 – 292, 2018.
- [39] Haipeng Xiong and Angela Yao. Discrete-constrained regression for local counting models. *2022 European Conference on Computer Vision (ECCV)*, 2022.
- [40] Shuo Yang, Hung-Ting Su, Winston H. Hsu, and Wen-Chin Chen. Class-agnostic few-shot object counting. *2021 IEEE Winter Conference on Applications of Computer Vision (WACV)*, pages 869–877, 2021.
- [41] Zhiyuan You, Yujun Shen, Kai Yang, Wenhan Luo, X. Lu, Lei Cui, and Xinyi Le. Few-shot object counting with similarity-aware feature enhancement. In *WACV*, 2023.
- [42] Zhiyuan You, Kai Yang, Wenhan Luo, Xin Lu, Lei Cui, and Xinyi Le. Few-shot object counting with similarity-aware feature enhancement. In *Proceedings of the Winter Conference on Applications of Computer Vision (WACV)*, 2023.
- [43] Anran Zhang, Lei Yue, Jiayi Shen, Fan Zhu, Xiantong Zhen, Xianbin Cao, and Ling Shao. Attentional neural fields for crowd counting. *2019 IEEE/CVF International Conference on Computer Vision (ICCV)*, pages 5713–5722, 2019.
- [44] Cong Zhang, Hongsheng Li, Xiaogang Wang, and Xiaokang Yang. Cross-scene crowd counting via deep convolutional neural networks. *2015 IEEE Conference on Computer Vision and Pattern Recognition (CVPR)*, pages 833–841, 2015.
- [45] Qi Zhang and Antoni Chan. Calibration-free multi-view crowd counting. *2022 European Conference on Computer Vision (ECCV)*, 2022.
- [46] Yingying Zhang, Desen Zhou, Siqin Chen, Shenghua Gao, and Yi Ma. Single-image crowd counting via multi-column convolutional neural network. In *CVPR*, pages 3754–3762, 2016.